# Broadband source of polarization entangled photons

A. Fraine,[1,*] O. Minaeva,[2] D. S. Simon,[1,3] R. Egorov,[1] and A. V. Sergienko[1,4,5]

[1]*Department of Electrical and Computer Engineering, Boston University, 8 Saint Mary's St., Boston, Massachusetts 02215, USA*

[2]*Department of Biomedical Engineering, Boston University, 44 Cummington St., Boston, Massachusetts 02215, USA*

[3]*Department of Physics and Astronomy, Stonehill College, 320 Washington St., Easton, Massachusetts 02357, USA*

[4]*Photonics Center, Boston University, Boston University, 8 Saint Mary's St., Boston, Massachusetts 02215, USA*

[5]*Department of Physics, Boston University, 590 Commonwealth Ave., Boston, Massachusetts 02215, USA*

*\*Corresponding author: afraine@bu.edu*

A broadband source of polarization entangled photons based on type-II spontaneous parametric down conversion from a chirped PPKTP crystal is presented. With numerical simulation and experimental evaluation, we report a source of broadband polarization entangled states with a bandwidth of approximately 125 nm for use in quantum interferometry. The technique has the potential to become a basis for the development of flexible broadband sources with designed spectral properties.   © 2012 Optical Society of America

*OCIS codes:*   270.4180, 230.4320.

A challenge in high resolution quantum interferometry is the production of high quality broadband polarization entangled states. In the past, broad spectra have been produced with thin crystals since the bandwidth of the spontaneous parametric down conversion (SPDC) spectrum is inversely proportional to the length of the crystal [1]. Several other techniques have been developed to create broad spectra from SPDC, such as chirped periodic poling for type-I interactions [2–4]. In addition, chirped quasi-phase matching has been used in second harmonic generation for pulse compression [5] and for designing optical parametric amplifiers [6]. However, the implementation of chirped periodically poled structures for type-II SPDC for the production of polarization entangled states has not been heavily studied. In comparison with previously studied type-I chirped periodically poled crystals, it is a greater challenge when working with type-II interactions since the SPDC spectrum is naturally more narrow. Despite this challenge, collinear type-II SPDC is a convenient source of polarization entanglement without any special state preparation needed other than a single beam splitter and coincidence detection.

Varying the phase matching period along the length of the crystal allows for multiple phase matching configurations to be realized in a single pass through the crystal resulting in a broad output spectrum. In this Letter, we describe the design and evaluation of a chirped PPKTP crystal (KTiOPO$_4$) as a source of broadband polarization entangled states with a bandwidth of approximately 125 nm.

By considering the crystal as a superposition of distributed sources along the propagation direction whose lengths vary linearly as illustrated in the inset of Fig. 1, one can calculate the SPDC spectrum as the sum of contributions from a sequence of smaller crystals of lengths $L_j = \frac{p_0}{2}\left(1 + \frac{\Delta p}{L_c}(z_j - z_0)\right)$ with $j \in [1, N]$, where $N$ is the number of distributed sources, $p_0$ is the degenerate phase matching period given by $p_0 = 2\lambda_p/(2n_p(\lambda_p) - n_s(2\lambda_p) - n_i(2\lambda_p))$, $\Delta p$ is a chirping parameter, $z_j$ is the location of the $j$th source, and $z_0$ is the location of $p_0$ along the propagation axis. For example, a chirped crystal with 20% chirping and $p_0$ located in the center of the crystal

has parameters $\Delta p = 0.2$ and $z_0 = L_c/2$, where $L_c$ is the total length of the crystal.

Assuming a plane wave pump and considering only the collinear signal and idler modes, the joint spectrum of SPDC photons is proportional to the Fourier transform of the longitudinally varying second order nonlinear coefficient. Following the procedure from [7], we can write

$$\tilde{\chi}^{(2)}(\omega_s, \omega_p - \omega_s) = \chi_0 \sum_{j=1}^{N} (-1)^j L_j \, \mathrm{sinc}(L_j \Delta k/2)$$
$$\times e^{-i\Delta k\left(L_j/2 + \sum_{k=j+1}^{N} L_k\right)}, \qquad (1)$$

where $\Delta k = k_p(\omega_p) - k_s(\omega_s) - k_i(\omega_p - \omega_s)$. The spectrum results from a superposition of single crystal spectra, which is evident from the sum of sinc functions. Because of a position dependent spectral phase, the output spectrum will have "bumpy" features due to interference from spectral components born at different locations in the crystal. The measured tuning curves displaying the spatial and spectral structure of a chirped PPKTP crystal with $\Delta p = 0.2$ and $z_0 = L_c/2$ are shown in Fig. 2. As a
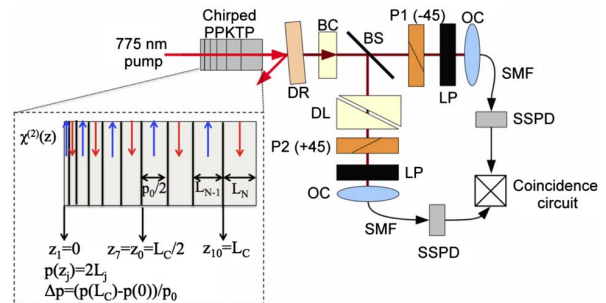


Fig. 1.   (Color online) Schematic of a polarization interferometer. The inset is a geometrical description of the linearly chirped periodically poled crystal. DR, dichroic reflector; BC, birefringent compensation; BS, beam splitter; P1/P2, polarizers; OC, optical coupler; SMF, single mode fiber; SSPD, superconducting photon detector; DL, birefringent delay line; LP, long pass filter.
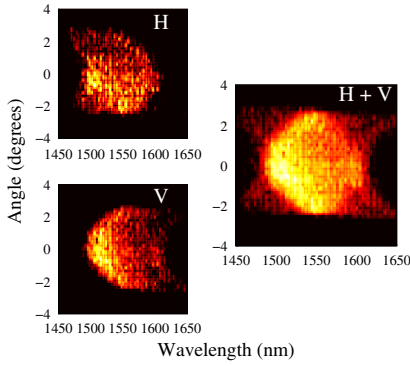
Fig. 2.   (Color online) Measured tuning curves for each polarization separately as well as overlapped from a chirped crystal with $\Delta p = 0.2$ and $z_0 = L_c/2$.

comparison, the tuning curve with temperature dependence for a nonchirped crystal designed for SPDC at 1550 nm from a 10 mm PPKTP crystal is shown in Fig. 3. The temperature dependence shows the absence of lateral walk-off present in birefringent phase matched bulk crystals.

To analyze the quantum properties of the SPDC photons, we use the polarization quantum interferometer described in [1,8–11] shown in Fig. 1. The two-photon wave function generated from SPDC is given by $|\Psi\rangle = \int d\omega \tilde{\chi}^{(2)}(\omega, \omega_p - \omega) \hat{a}_s^\dagger(\omega) \hat{a}_i^\dagger(\omega_p - \omega)|0\rangle$. The form of the wave function is determined by the spectral function, which is controlled by the Fourier transform of the nonlinear coefficient in Eq. (1).

Following the procedure from [9–11], the coincidence rate is written as the difference between a constant background term and an interference term written as $R(L_b) \propto R_0 - R_{int}(L_b)$, where $R_0$ is the background term,

$$R_{int}(L_b) = \int d\omega \Phi(\omega, \omega_p - \omega) \Phi^*(\omega_p - \omega, \omega)$$
$$\times [e^{i \Delta n_b(\omega) \omega L_b/c} + e^{i \Delta n_b(\omega_p - \omega)(\omega_p - \omega) L_b/c}], \quad (2)$$

$L_b$ is the length of the birefringent delay line, and $\Delta n_b(\omega)$ is the difference between the signal and idler indices of refraction at frequency $\omega$ in the birefringent delay line.

The calculated coincidence rates and spectra from a linearly chirped crystal with $\Delta p = 0.2$, $z_0 = L_c/2$, $L_c = 10$ mm, and $\lambda_p = 775$ mm for three different temperatures are shown in Fig. 4. As expected, there is significant beating in the interference profile due to spectral profile modulation as a result of interference between spectral components originating from different longitudinal positions. However, the main feature of the interfer-
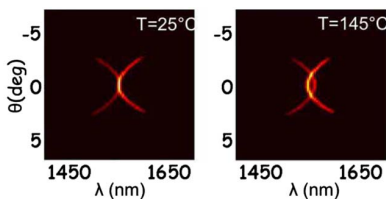


Fig. 3.   (Color online) Measured tuning curves for a nonchirped crystal.
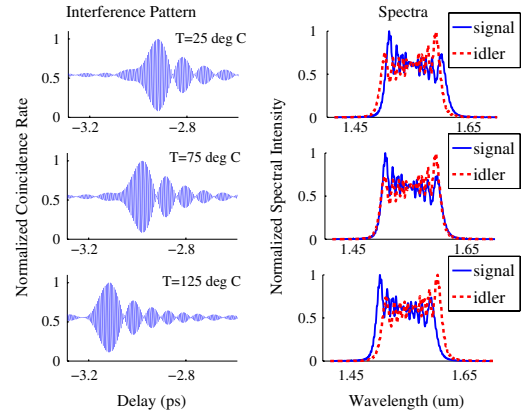


Fig. 4.   (Color online) Calculation of the interference patterns as well as signal (solid line) and idler (dotted line) spectra at three different temperatures. The time delay axis of the interference patterns corresponds to the differential group delay between the two polarization modes that is scanned by a moving a pair of quartz wedges in one of the arms. The peak of the interferograms corresponds to the differential group delay from the chirped PPKTP crystal itself.

ence function that is used in quantum metrology is the central peak. As long as this peak is sufficiently narrow to achieve the desired resolution, the adjacent features are inconsequential.

Despite this, it is often desirable to have a central peak that is unobstructed by any auxiliary features such as those due to beating. It is shown in Fig. 4 that the temperature of the crystal can be a controlling parameter that can be used to optimize the central feature to make it more suitable for a particular type of measurement. Although the amount of spectral overlap does not significantly change in a relatively large range of temperatures, the beating does not obstruct the central peak for $T = 125\,°C$, making the feature more precisely defined. Furthermore, it is clear that as the temperature is increased, the main feature becomes more isolated and thus more suitable for use in high resolution quantum interferometry. The less than 100% visibility is a direct result of partial spectral distinguishability between polarizations.

To probe the nature of polarization entanglement, we use the polarization quantum interferometer shown in Fig. 1. The 775 nm pump from a CW Ti:Sapphire laser with power of 1 W is focused by a 300 mm focal length lens into the chirped PPKTP crystal, which is situated in a temperature stabilized oven. The SPDC photons centered around 1550 nm pass through a dichroic reflector, which rejects the pump wavelength, pass through a birefringent element to compensate for the longitudinal walk-off from the crystal, and form a superposition by a 50/50 polarization-insensitive beam splitter. One path contains a birefringent delay line, which delays one polarization relative to the other. In principle, the birefringent element before the beam splitter is not necessary since the longitudinal walk-off from the crystal can be compensated in the postponed delay line; however, the delay line was not long enough to completely compensate the crystal birefringence, so an extra fixed delay was added before the beam splitter for convenience. Each path contains a polarizer oriented
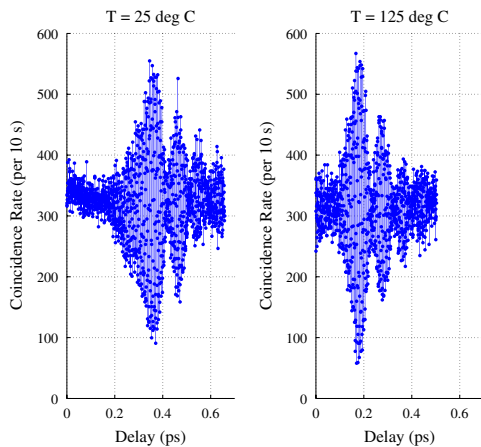
Fig. 5. (Color online) Quantum interferograms obtained from the setup described in Fig. 1. These results agree well with the results of numerical calculations shown in Fig. 4. When used in quantum interferometry, the relevant measurement is the shift in the interference feature rather than the absolute position, since this is made arbitrary by the birefringent compensating element before the beam splitter.

at $\pm 45°$ with respect to the polarization basis to ensure indistinguishability. The photons are coupled into single mode fibers and detected in coincidence with a 2 ns coincidence window to post select the polarization entangled state using two superconducting single photon detectors (SSPDs) with quantum efficiencies of 7% at 1550 nm, a dark count rate of approximately 100 counts/s, and temporal a resolution of 50 ps. The accidental coincidence rate was $2\ \mathrm{s}^{-1}$, and the single rates in each detector were approximately $2 \times 10^4\ \mathrm{s}^{-1}$.

The interferograms were recorded at $T = 25\,°\mathrm{C}$ and $T = 125\,°\mathrm{C}$, shown in Fig. 5 agreeing closely with the simulations shown in Fig. 4.

Several issues must be addressed when designing chirped periodically poled crystals for the production of high quality polarization entangled states over a broad spectral range. First, there must be spectral indistinguishability between the two polarization modes in order to maximize the visibility of the interference features. Second, the shape of the interference feature is directly related to the shape of the spectra. Therefore, to get a smooth and well defined interference feature, which is necessary to make high resolution measurements, one must address the specific shape of the spectra by designing appropriate chirping schemes or controlling external parameters of the system, such as temperature, pump wavelength, and chirping parameters.

In addition to using type-II SPDC to produce polarization entangled states, it should be noted that type-I SPDC can be manipulated to produce polarization entangled states with the appropriate post selection as well. By splitting the collinear polarization-degenerate photons from a chirped type-I nonlinear crystal with a beam splitter, rotating the polarization in one arm by 90° and recombining with a second beam splitter, a similar polarization entangled state to the one described in this report can be achieved. This technique will benefit from higher spectral indistinguishability, but will likely suffer from lower stability due to the reliance on interferometric alignment.

The linearly chirped type-II PPKTP crystal has proven to be a convenient source of broadband polarization entanglement with a central wavelength of 1550 nm, which is within the main telecom window. This has been useful for high resolution quantum interference measurements specifically for the precise evaluation of polarization group delays [11].

## References

1. E. Dauler, G. Jaeger, A. Muller, A. L. Migdall, and A. V. Sergienko, J. Res. Natl. Inst. Stand. Technol. **104**, 1 (1999).
2. S. Carrasco, M. Nasr, A. V. Sergienko, B. Saleh, M. C. Teich, J. P. Torres, and L. Torner, Opt. Lett. **31**, 253 (2006).
3. M. Nasr, S. Carrasco, B. Saleh, A. V. Sergienko, M. C. Teich, J. P. Torres, L. Torner, D. Hum, and M. Fejer, Phys. Rev. Lett **100**, 183601 (2008).
4. S. Carrasco, J. P. Torres, L. Torner, A. V. Sergienko, B. Saleh, and M. C. Teich, Opt. Lett. **29**, 2429 (2004).
5. M. A. Arbore, O. Marco, and M. M. Fejer, Opt. Lett. **22**, 865 (1997).
6. M. Charbonneau-Lefort, B. Afeyan, and M. M. Fejer, J. Opt. Soc. Am. B **25**, 463 (2008).
7. G. DiGiuseppe, M. Atature, M. D. Shaw, A. V. Sergienko, B. Saleh, and M. C. Teich, Phys. Rev. A **66**, 013801 (2002).
8. T. B. Pittman, D. V. Strekalov, A. Migdall, M. H. Rubin, A. V. Sergienko, and Y. H. Shih, Phys. Rev. Lett. **77**, 1917 (1996).
9. D. Branning, A. L. Migdall, and A. V. Sergienko, Phys. Rev. A **62**, 063808 (2000).
10. A. Fraine, D. S. Simon, O. Minaeva, R. Egorov, and A. V. Sergienko, Opt. Express **19**, 22820 (2011).
11. A. Fraine, O. Minaeva, D. S. Simon, R. Egorov, and A. V. Sergienko, Opt. Express **20**, 2025 (2012).